Analytical Modeling of Mass and Heat Transfer on Unsteady Squeezing Viscous Nanofluid Flow under the Influence of Slip Velocity

Renna D. Abdul-Wahhab ، Abeer Majeed Jasim
Department of Mathematics, College of science, University of Basrah, Basrah, Iraq

Abstract:

In this article, two-dimensional unsteady incompressible viscous nanofluids magneto-hydrodynamic (MHD) flow among two parallel plates extended infinitely is investigated. The equations that results from the use of similarity transformations for non-linear partial differential system are solved by the new algorithm. The important key to this construct is the derivatives that appear as coefficients in the power series. The effects of apparent physical parameters on velocity concentration and temperature distributions are described using a schematic diagram and interpreted physically. The effects of apparent physical parameters on concentration, temperature, and velocity distributions are described by graphs. For the flow of nanofluids, the results indicate that it is inversely proportional between the rate of mass and heat transfer with nanoparticle size fraction and magnetic parameter. Over time, squeeze number and schmidt number lead to increase the rate of mass transfer. This problem is dissolved numerically by using the Runge-Kutta scheme of fourth-order (RK4S) .

النمذجة التحليلية لانتقال الكتلة والحرارة على مسائلة الموائع النانوية للتدفق اللزج غير المستقر تحت تأثير سرعة الانزلاق

رنا عبد الوهاب ، عبير مجيد جاسم
قسم الرياضيات ، كلية العلوم، جامعة البصره، البصره، العراق

الخلاصة

في هذه المقالة ، يتم فحص تدفق اللزوجة غير المستقرة وغير القابلة للضغط من السوائل النانوية بين لوحين متوازيين ممتدين بشكل لا نهائي. يتم حل معادلات النتائج من استخدام تحويلات التشابه للنظام التفاضلي الجزئي غير الخطي بواسطة الخوارزمية الجديدة. المفتاح المهم لهذا البناء هو المشتقات التي تظهر كمعاملات في متسلسلة القوة. يتم وصف تأثيرات المعلمات الفيزيائية الظاهرة على تركيز السرعة وتوزيعات درجة الحرارة باستخدام رسم تخطيطي وتفسير فيزيائي . بالنسبة لتدفق السوائل النانوية ، تشير النتائج إلى وجود تناسق عكسي بين معدل الكتلة ونقل الحرارة مع جزء حجم الجسيمات النانوية والمعلمة المغناطيسية. ظط دد الاط المسائلة باستخدام مخطط رنج كتا.

*Email: rana.abdul_wahhab@uobasrah.edu.iq

Introduction:

The analysis of mass and heat transfer for a viscid nano-fluid an unsteady flow among two parallel plates is motivational topic for reconnaissance cause of their industrial use and biological conditions, Its many physical and engineering applications can be described by Figure1. As follows:
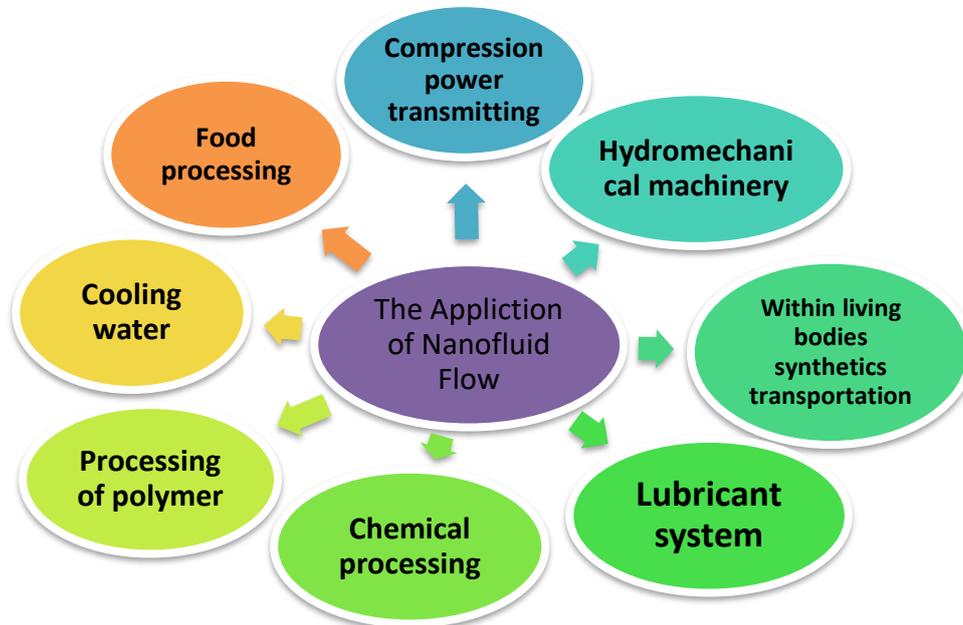

Figure1: The Application of Nanofluid Flow.

Stefan [1] was the first to **st**udy the squeeze flow under lubrication approximation. The problem of a compressed nano-fluid an unsteady flow among two parallel plates has been suggested by Gupta and Ray [2]. The term nano-fluid is first proposed by Choi a]]]]]\nd Eastman [3] a fluid in which nanoparticles are postponed in an improper fluid such as oil, ethylene glycol, and water with low thermal conductivity. For Cu / water and Cu/ kerosene the squeezing flow of nano-fluid among two parallel plates under the impacts of velocity slip and the dissipation of viscous was studied by Khan et al [4]. Khilap et al.[5] have acquired an analytic approximate solution for squeezing nano-fluid flow. In the base fluid, a nanofluid displays a fluid that is particles size on the order of a nanometer where diameter less of 100 nm are combined. Usually, the conduction of fluid for the base fluid is a for example as lubricants, oils, polymer solution, water 5%, ethylene glycol, water, toluene, and bio-fluids. In nanofluids, nanoparticles are existing in active to of the fraction volume. Because nanofluids have a high heat transfer capacity, they have better property than conventional heat transfer fluids which are poor in heat conduction. For energy supply, Cooling and heating fluids display an important role in developing energy efficient equipment heat transfer. Therefore, nano-sized conductive metal particles were added to rise the thermal conductivity of these fluids. Moreover, the importance of these fluids is efficient use in modern industry, and important applications of these nanofluid are microelectronics, pharmaceutical processes and fuel cells. In recent years, many authors have reported and studied nanofluid technology analytically, numerically, experimentally in the presence of heat transfer [6-17]. The algorithm of the present study is to account for mass transfer, heat transfer and the slip velocity on unsteady squeezing nanofluid flow among two parallel plates. In this work, we employed a new algorithm and Runge-Kutta 4-order (RK4S) scheme and shooting scheme to discover the analytical and numerical solutions respectively of nonlinear ordinary differential equations. The impacts of governing physical parameters such as nanoparticle volume

fraction, Schmidt number squeeze number, magnetic and slip parameter on concentration, temperature, and velocity, as well as on Sherwood number, Nusselt, and skin-friction coefficient are examined. From our simple information, in the scientific literature this research has not been studied.

The Statement of Problem:

Mass and heat transfer of two dimensional an unsteady squeezing nano-fluid in the middle are two parallel plates which infinite expansion. The distance between two plates can be define as $y = \pm h(t) = \pm J(1 - \xi t)^{0.5}$, when time $t = 0, J$ is the initial position . In this system, the flow does not have a chemical reaction, incompressible, the effects of viscous dissipation are preserved. For both the plates in direction perpendicular a transverse magnetic field of flexible strength is forced. Graphical modeling [6] for this study is presented see Figure.2.
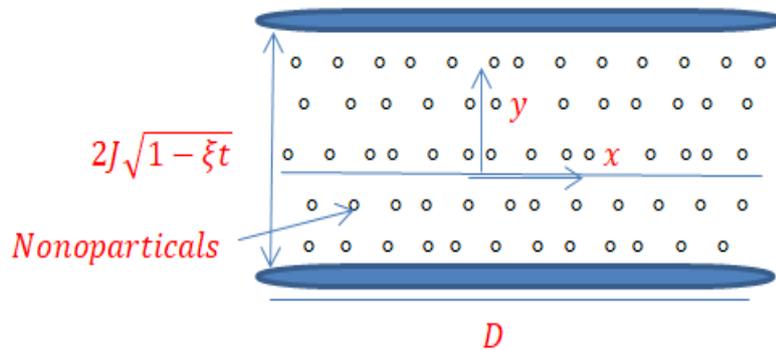
Figure 2: The Configuration of Flow.

This problem representing nanofluid flow is as follows:

$$\frac{\partial \breve{u}}{\partial x} + \frac{\partial \breve{v}}{\partial y} = 0, \tag{1}$$

$$\frac{\partial \breve{u}}{\partial t} + \breve{u}\frac{\partial \breve{u}}{\partial x} + \breve{v}\frac{\partial \breve{u}}{\partial y} + \frac{1}{\breve{\rho}_{nf}}\frac{\partial \breve{p}}{\partial x} - \frac{\breve{\mu}_{nf}}{\breve{\rho}_{nf}}\left[\frac{\partial^2 \breve{u}}{\partial x^2} + \frac{\partial^2 \breve{u}}{\partial y^2}\right] + \breve{\sigma}_{nf}\breve{B}_0\breve{u} = 0, \tag{2}$$

$$\frac{\partial \breve{v}}{\partial t} + \breve{u}\frac{\partial \breve{v}}{\partial x} + \breve{v}\frac{\partial \breve{v}}{\partial y} + \frac{1}{\breve{\rho}_{nf}}\frac{\partial \breve{p}}{\partial y} - \frac{\breve{\mu}_{nf}}{\breve{\rho}_{nf}}\left[\frac{\partial^2 \breve{v}}{\partial x^2} + \frac{\partial^2 \breve{v}}{\partial y^2}\right] = 0, \tag{3}$$

$$\frac{\partial \breve{T}}{\partial t} + \breve{u}\frac{\partial \breve{T}}{\partial x} + \breve{v}\frac{\partial \breve{T}}{\partial y} - \frac{\breve{k}_{nf}}{(\breve{\rho}\,\breve{C}_{\breve{p}})_{nf}}\left[\frac{\partial^2 \breve{T}}{\partial x^2} + \frac{\partial^2 \breve{T}}{\partial y^2}\right] - \frac{\breve{\mu}_{nf}}{(\breve{\rho}\,\breve{C}_{\breve{p}})_{nf}}\left[4\left(\frac{\partial \breve{u}}{\partial x}\right)^2 + \left(\frac{\partial \breve{u}}{\partial y} + \frac{\partial \breve{u}}{\partial x}\right)^2\right] = 0, \tag{4}$$

$$\frac{\partial \breve{c}}{\partial t} + \breve{u}\frac{\partial \breve{c}}{\partial x} + \breve{v}\frac{\partial \breve{c}}{\partial y} - D\left[\frac{\partial^2 \breve{c}}{\partial x^2} + \frac{\partial^2 \breve{c}}{\partial y^2}\right] = 0, \tag{5}$$

The components of the velocity are $\breve{u}$ and $\breve{v}$. $\breve{T}, \breve{p}, \breve{\rho}_{nf}, (\breve{\rho}\,\breve{C}_{\breve{p}})_{nf}$ and $\breve{\mu}_{nf}$ indicate the temperature, the pressure, density, heat capacitance, and dynamic viscosity. The stated problem has the boundary conditions given form

$$\breve{u} = -\breve{L}\frac{\partial \breve{u}}{\partial y}, \breve{v} = \breve{v}_w = \frac{dh}{dt}, \breve{T} = \breve{T}_h, \breve{C} = \breve{C}_h \text{ at } y = h(t), \tag{6}$$

$$\breve{v} = \frac{\partial \breve{u}}{\partial y} = \frac{\partial \breve{T}}{\partial y}, \breve{C} = \breve{C}_0 \text{ at } y = 0, \tag{7}$$

The mathematics equation of the nanofluid are :

- The density : $\breve{\rho}_{nf} = (1 - \Delta)\breve{\rho}_f + \Delta\,\breve{\rho}_{s,}$
- The heat capacity : $(\breve{\rho}\,\breve{C}_{\breve{p}})_{nf} = (1 - \Delta)(\breve{\rho}\,\breve{C}_{\breve{p}})_f + \Delta(\breve{\rho}\,\breve{C}_{\breve{p}})_{s,}$
- The dynamic viscosity (Brinkman) : $\breve{\mu}_{nf} = \frac{\breve{\mu}_f}{(1-\Delta)^{2.5}}$,

- The thermal conductivity (Maxwell-Garnetts): $\breve{k}_{nf} = \frac{\breve{k}_s + 2\breve{k}_f - 2\Delta(\breve{k}_f - \breve{k}_s)}{\breve{k}_s + 2\breve{k}_f + 2\Delta(\breve{k}_f - \breve{k}_s)} \breve{k}_f$,

$\breve{k}_s, \breve{k}_f, \breve{\rho}_f, \Delta$ and $\breve{\rho}_s$ are the thermal conductivity for the solids, the thermal conductivity for of the base fluid, the fluid density, volume fraction of nanoparticles and the density of the solid respectively. Equations.1-7 can be simplified through the following definitions:

$$\breve{u} = \frac{\alpha x}{l(1-\xi t)} \mathrm{M}'(\alpha), \breve{v} = -\frac{\alpha l}{2(1-\xi t)^{0.5}} \mathrm{M}(\alpha), \alpha = \frac{y}{l(1-\xi t)^{0.5}}, \tag{a8}$$

$$Z(\alpha) = \frac{\breve{T} - \breve{T}_0}{\breve{T}_h - \breve{T}_0}, E(\alpha) = \frac{\breve{C} - \breve{C}_0}{\breve{C}_h - \breve{C}_0}, \tag{b8}$$

$\mathrm{M}'(\alpha)$ is the velocity distribution along the x-axis, $\mathrm{M}(\alpha)$ is the velocity distribution along the y-axis, $Z(\alpha)$ is dimensionless temperature distribution , $E(\alpha)$ is dimensionless concentration function and α is the local similarity variable. Now, substituting Equation .a8 and Equation. b8 into Equations .1-7. The final from of the resulting equations are

$$\frac{d^4\mathrm{M}}{d\alpha^4} - Sf_1(1-\Delta)^{2.5} \left[\alpha \frac{d^3\mathrm{M}}{d\alpha^3} + 3\frac{d^2\mathrm{M}}{d\alpha^2} + \frac{d\mathrm{M}}{d\alpha}\frac{d^2\mathrm{M}}{d\alpha^2} - \mathrm{M}\frac{d^3\mathrm{M}}{d\alpha^3}\right] - kn\frac{d^2\mathrm{M}}{d\alpha^2} = 0, \tag{9}$$

$$\frac{d^2Z}{d\alpha^2} + \frac{\Pr S f_2}{f_3}\left[\mathrm{M}\frac{dZ}{d\alpha} - \alpha \frac{dZ}{d\alpha}\right] + \frac{\Pr Ec}{f_3(1-\Delta)^{2.5}}\left[\left(\frac{d^2\mathrm{M}}{d\alpha^2}\right)^2 + 4\psi^2(\frac{d\mathrm{M}}{d\alpha})^2\right] = 0, \tag{10}$$

$$\frac{d^2E}{d\alpha^2} + S\,Sc\left[\mathrm{M}\frac{dE}{d\alpha} - \alpha \frac{dE}{d\alpha}\right] = 0, \tag{11}$$

The boundary conditions provided are

$$\mathrm{M}(0) = 0, \frac{d^2\mathrm{M}(0)}{d\alpha^2} = 0, \frac{d\mathrm{M}(0)}{d\alpha} = 0, E(0) = 0, \tag{a12}$$

$$\mathrm{M}(1) = 0, \frac{d\mathrm{M}(1)}{d\alpha} = -\Omega \frac{d^2\mathrm{M}(1)}{d\alpha^2}, Z(1) = 1, E(1) = 1, \tag{b12}$$

The definitions of the parameters for Equations .9-12 as

Schmidt parameter: $Sc = \frac{v_f}{D_{nf}}$, Squeeze parameter: $S = \frac{\xi l^2}{2v_f}$, Prandtl parameter: $Pr = \frac{\breve{\mu}_f(\breve{C}_{\breve{p}})_f}{\breve{k}_f}$, Eckert parameter: $Ec = \frac{\breve{\rho}_f}{(\breve{\rho}\,\breve{C}_{\breve{p}})_f}\left(\frac{\xi x}{2(1-\xi t)}\right)^2$, Slip parameter: $\Omega = \frac{L}{l(1-\xi t)^{0.5}}$, The reference length: $\psi = \frac{1}{x}$, The magnetic parameter : $kn = \frac{2\breve{\sigma}_{nf}\breve{B}_0{}^2 h(t)^2}{\breve{\mu}_f \breve{\rho}_f}$,

The proposed system has been implanted nanofluid where to appear the base fluid which is water contains various kinds of nanoparticles such as silver (Ag), titanium oxide (TiO2), alumina (Al2O3) and copper Cu with addition the slip velocity under effect . The properties of thermo physical nano-fluids are introduced in Table 1.

Table 1: The properties of hermo physical nano-fluids.

Thermo physical Properties	$\breve{\rho}\,(\frac{Kg}{m^3})$	$\breve{C}_{\breve{p}}\,(\frac{J}{kgK})$	$\breve{k}(\frac{W}{mK})$
Pure water	997.1	4179	0.613
Cu	8933	385	401
Ag	10500	235	429
Al2O3	3970	765	40
TiO2	4250	686.2	8.9538

The Physical of Quantities:

the Sherwood number S_{hx} , the Nusselt number N_{ux} and the skin friction coefficient C_{fx} can be introduced as

$$S_{hx} = \frac{l\,m_w}{D_{nf}(\breve{C}_h - \breve{C}_0)}, m_w = -D_{nf}\left(\frac{\partial\breve{C}}{\partial y}\right)_{y=h(t)}, \tag{a13}$$

$$N_{ux} = \frac{l\,q_w}{\breve{k}_f(\breve{T}_h - \breve{T}_0)}, q_w = -\breve{k}_{nf}\left(\frac{\partial\breve{T}}{\partial y}\right)_{y=h(t)}, \tag{b13}$$

$$C_{fx} = \frac{\tau_w}{\breve{\rho}_{nf}v_w^2}, \tau_w = \breve{\mu}_{nf}\left(\frac{\partial\breve{u}}{\partial y}\right)_{y=h(t)}, \tag{c13}$$

By using Equation .8 and Equation.13, yield

$$S_{hx}^* = \sqrt{1 - \xi t}\, S_{hx} = -\frac{dE(1)}{d\alpha}, \tag{14}$$

$$N_{ux}^* = \sqrt{1 - \xi t}\, N_{ux} = -f_3 \frac{dZ(1)}{d\alpha}, \tag{15}$$

$$C_{fx}^* = \left(\frac{1}{f_1(1-\epsilon)^{\frac{5}{2}}}\right)\frac{d^2 M(1)}{d\alpha^2}, \tag{16}$$

where R_{ex} is Reynolds number.

The Application of New Algorithm for Squeezing Unsteady Magneto-hydrodynamic Nano-Fluid Flow Problem:

In this section, the steps of the new algorithm[6-10] are implemented to resolve the ordinary differential Equations .9 - 12 to find the analytic approximate solution $M(\alpha)$, $Z(\alpha)$, and $E(\alpha)$, can be summarized, by integrating Equation .9 four times, Equation.10 and Equation .11 twotimes with respect to α in $[0, \alpha]$, we get

$$M(\alpha) = J_{11} + J_{12}\alpha + J_{13}\frac{\alpha^2}{2!} + J_{14}\frac{\alpha^3}{3!} + L_1^{-1}[Sf_1(1-\Delta)^{2.5}(\alpha\frac{d^3 M}{d\alpha^3} + 3\frac{d^2 M}{d\alpha^2} + \frac{dM}{d\alpha}\frac{d^2 M}{d\alpha^2} -$$

$$M\frac{d^3 M}{d\alpha^3}) + kn\frac{d^2 M}{d\alpha^2}], \tag{a17}$$

$$Z(\alpha) = J_{21} + J_{22}\alpha - L_2^{-1}[\frac{\Pr S f_2}{f_3}\left(M\frac{dZ}{d\alpha} - \alpha\frac{dZ}{d\alpha}\right) + \frac{\Pr Ec}{f_3(1-\Delta)^{2.5}}(\left(\frac{d^2 M}{d\alpha^2}\right)^2 + 4\psi^2 \left(\frac{dM}{d\alpha}\right)^2)], \tag{b17}$$

$$E(\alpha) = J_{31} + J_{32}\alpha - L_3^{-1}[S\, Sc\left(M\frac{dE}{d\alpha} - \alpha\frac{dE}{d\alpha}\right)], \tag{c17}$$

the Equations .a17-c17 become by formula as follow:

$$M(\alpha) = J_{11} + J_{12}\alpha + J_{13}\frac{\alpha^2}{2!} + J_{14}\frac{\alpha^3}{3!} + L_1^{-1}K_1[H(\alpha)], \tag{18a}$$

$$Z(\alpha) = J_{21} + J_{22}\alpha + L_2^{-1}K_2[Z(\alpha)], \tag{18b}$$

$$E(\alpha) = J_{31} + J_{32}\alpha + L_3^{-1}K_3[E(\alpha)], \tag{18c}$$

whereas,

$J_{11} = M(0), J_{12} = M'(0), J_{13} = M''(0), J_{14} = M'''(0), J_{21} = Z(0), J_{22} = Z'(0),$
$J_{31} = E(0), J_{32} = E'(0),$ and $L_1^{-1} = \int_0^\alpha \int_0^\alpha \int_0^\alpha \int_0^\alpha (.)(d\alpha)^4$, $L_2^{-1} = L_3^{-1} = \int_0^\alpha \int_0^\alpha (.)(d\alpha)^2$,

$$K_1[M(\alpha)] = Sf_1(1-\Delta)^{2.5}\left[\alpha\frac{d^3 M}{d\alpha^3} + 3\frac{d^2 M}{d\alpha^2} + \frac{dM}{d\alpha}\frac{d^2 M}{d\alpha^2} - M\frac{d^3 M}{d\alpha^3}\right] + kn\frac{d^2 M}{d\alpha^2},$$

$$K_2[Z(\alpha)] = -\frac{\Pr S f_2}{f_3}\left[M\frac{dZ}{d\alpha} - \alpha\frac{dZ}{d\alpha}\right] - \frac{\Pr Ec}{f_3(1-\Delta)^{2.5}}[\left(\frac{d^2 M}{d\alpha^2}\right)^2 + 4\psi^2(\frac{dM}{d\alpha})^2],$$

$$K_3[E(\alpha)] = -S\, Sc\left[M\frac{dE}{d\alpha} - \alpha\frac{dE}{d\alpha}\right],$$

form boundary conditions Equation .12a and Equation.12b become

$$M(\alpha) = J_{12}\alpha + J_{14}\frac{\alpha^3}{3!} + L_1^{-1}K_1[M(\alpha)], \tag{19a}$$

$$Z(\alpha) = J_{21} + L_2^{-1}K_2[Z(\alpha)], \tag{19b}$$

$$E(\alpha) = J_{32}\alpha + L_3^{-1}K_3[E(\alpha)], \tag{19c}$$

with the following hypothesis:

$$K_1[M(\alpha)] = \sum_{m=1}^\infty \frac{d^{(m-1)}K_1[M_0(\alpha)]}{d\alpha^{(m-1)}}, \quad K_2[Z(\alpha)] = \sum_{m=1}^\infty \frac{d^{(m-1)}K_2[Z_0(\alpha)]}{d\alpha^{(m-1)}},$$

$$K_3[E(\alpha)] = \sum_{m=1}^\infty \frac{d^{(m-1)}K_3[E_0(\alpha)]}{d\alpha^{(m-1)}}, \tag{20}$$

Through the above hypotheses, we find that the analytical solutions is known as the following as:

$$M(\alpha) = M_0 + M_1 + M_2 + \cdots, \tag{21a}$$

$$Z(\alpha) = Z_0 + Z_1 + Z_2 + \cdots, \tag{21b}$$

$$E(\alpha) = E_0 + E_1 + E_2 + \cdots, \tag{21c}$$

so,

$M_0 = J_{12}\alpha + J_{14}\frac{\alpha^3}{3!}$, $M_1 = L_1^{-1}K_1[M_0(\alpha)]$, $M_2 = L_1^{-1}K_1'[M_0(\alpha)]$, ...,

$Z_0 = J_{21}$, $Z_1 = L_2^{-1}K_2[Z_0(\alpha)]$, $Z_2 = L_2^{-1}K_2'[Z_0(\alpha)]$, ...,

$E_0 = J_{32}\alpha$, $E_1 = L_3^{-1}K_3[E_0(\alpha)]$, $E_2 = L_3^{-1}K_3'[E_0(\alpha)]$, ...,

The values of K_1, K_2 and K_3 with derivatives with respect to α. Let can be calculate which is the crucial part of new algorithm:

$$K_1[M_0(\alpha)] = Sf_1(1-\Delta)^{2.5}\left[\alpha\frac{d^3M_0}{d\alpha^3} + 3\frac{d^2M_0}{d\alpha^2} + \frac{dM_0}{d\alpha}\frac{d^2M_0}{d\alpha^2} - M_0\frac{d^3M_0}{d\alpha^3}\right] + kn\frac{d^2M_0}{d\alpha^2}, \qquad (22)$$

$$K_2[Z_0(\alpha)] = -\frac{\Pr S f_2}{f_3}\left[M_0\frac{dZ_0}{d\alpha} - \alpha\frac{dZ_0}{d\alpha}\right] - \frac{\Pr Ec}{f_3(1-\Delta)^{2.5}}\left[\left(\frac{d^2M_0}{d\alpha^2}\right)^2 + 4\psi^2\left(\frac{dM_0}{d\alpha}\right)^2\right], \qquad (23)$$

$$K_3[E_0(\alpha)] = -S\,Sc\left[M_0\frac{dE_0}{d\alpha} - \alpha\frac{dE_0}{d\alpha}\right], \qquad (24)$$

$$K_1'[M_0(\alpha)] = \sum_{g_1=1}^{4} K_{1M_0}{}^{(g_1-1)}\cdot(M_{0\alpha})^{(g_1-1)}, \qquad (25)$$

$$K_2'[Z(\alpha)] = \sum_{g_1=1}^{3} K_{2M_0}{}^{(g_1-1)}\cdot(M_{0\alpha})^{(g_1-1)} + K_{2Z_0'}\cdot(Z_{0\alpha})', \qquad (26)$$

$$K_3'[E_0(\alpha)] = K_{3E_0'}\cdot(E_{0\alpha})' + K_{3M_0}M_{0\alpha}, \qquad (27)$$

$\vdots$

The derivatives of the functions M, Z and E are unknown. As wall as, we propose hypothesis as follows:

$$M_\alpha = M_1 = L^{-1}K_1[M_0(\alpha)], \quad M_{\alpha\alpha} = M_2 = L^{-1}K_1'[M_0(\alpha)], \qquad (28)$$

$$Z_\alpha = Z_1 = L^{-1}K_2[Z_0(\alpha)], \quad Z_{\alpha\alpha} = Z_2 = L^{-1}K_2'[Z_0(\alpha)], \qquad (29)$$

$$E_\alpha = E_1 = L^{-1}K_3[E_0(\alpha)], \quad E_{\alpha\alpha} = E_2 = L^{-1}K_3'[E_0(\alpha)], \qquad (30)$$

Now, the first derivatives of K as follows:

$k_{1M_0} = -Sf_1(1-\Delta)^{2.5}M_0''', k_{1M_0M_0} = k_{1M_0M_0'} = 0, k_{1M_0M_0'''} = -Sf_1(1-\Delta)^{2.5},$

$k_{1M_0M_0M_0} = k_{1M_0M_0M_0'} = k_{1M_0M_0'M_0'} = k_{1M_0M_0'M_0'} = k_{1M_0M_0''M_0''} = k_{1M_0M_0'''M_0'''} = 0,$

$k_{1M_0'} = Sf_1(1-\Delta)^{2.5}M_0'', k_{1M_0M_0'} = k_{1M_0'M_0'''} = 0, k_{1M_0'M_0''} = Sf_1(1-\Delta)^{2.5},$

$k_{1M_0M_0M_0'} = k_{1M_0M_0'M_0'} = k_{1M_0'M_0'M_0'} = k_{1M_0'M_0'''M_0'} = k_{1M_0'M_0''M_0''} = k_{1M_0'M_0'''M_0'''} = 0,$

$k_{1M_0''} = Sf_1(1-\Delta)^{2.5}(3 + M_0') + kn, k_{1M_0''M_0''} = 0, k_{1M_0''M_0'} = Sf_1(1-\Delta)^{2.5},$

$k_{1M_0''M_0M_0'} = k_{1M_0''M_0'M_0'} = k_{1M_0''M_0'M_0'} = k_{1M_0''M_0'''M_0'} = k_{1M_0''M_0''M_0''} = k_{1M_0''M_0'''M_0'''} = 0,$

$k_{1M_0'''} = Sf_1(1-\Delta)^{2.5}(\alpha - M_0), k_{1M_0'''M_0''} = 0, k_{1M_0'''M_0} = Sf_1(1-\Delta)^{2.5},$

$k_{1M_0'''M_0M_0'} = k_{1M_0'''M_0'M_0'} = k_{1M_0'''M_0'M_0'} = k_{1M_0'''M_0'''M_0'} = k_{1M_0'''M_0''M_0''} = k_{1M_0'''M_0''M_0'''} = 0,$

$K_{2M_0} = -\frac{\Pr S f_2}{f_3}Z_0', k_{2M_0M_0'} = k_{2M_0M_0''} = k_{2M_0M_0} = 0, K_{2M_0Z_0'} = -\frac{\Pr S f_2}{f_3},$

$k_{2g_0g_0g_0} = k_{2g_0g_0'g_0} = k_{2g_0g_0'g_0'} = k_{2g_0'g_0'''g_0'} = k_{2g_0g_0''g_0''} = k_{2g_0g_0'''g_0'''} = 0,$

$K_{2M_0'} = -\frac{2\Pr Ec}{f_3(1-\Delta)^{2.5}}M_0', k_{2M_0M_0'} = k_{2M_0'M_0'} = 0, K_{2M_0M_0'} = -\frac{2\Pr Ec}{f_3(1-\Delta)^{2.5}},$

$k_{2M_0'M_0M_0} = k_{2M_0M_0'M_0'} = k_{2M_0'M_0'M_0'} = k_{2M_0'Z_0'M_0'} = k_{2M_0'Z_0'Z_0'} = k_{2M_0'M_0''M_0'''} = 0,$

$K_{2M_0''} = \frac{-8\psi^2 P_r E_c}{f_3(1-\Delta)^{2.5}}M_0'', k_{2M_0''M_0'} = k_{2M_0''M_0''} = 0, K_{2M_0''M_0''} = \frac{-8\psi^2 P_r E_c}{f_3(1-\Delta)^{2.5}},$

$k_{2M_0'M_0Z_0'} = k_{2M_0M_0''M_0'} = k_{2M_0''M_0'''M_0'} = k_{2M_0''Z_0'M_0'} = k_{2M_0''M_0'\theta_0'} = k_{2M_0''M_0''M_0'''} = 0,$

$k_{2M_0'M_0Z_0'} = k_{2Z_0'M_0''M_0'} = k_{2Z_0'M_0''M_0'} = k_{2Z_0'Z_0'M_0'} = k_{2Z_0'Z_0'Z_0'} = k_{2M_0''M_0''M_0'''} = 0,$

$K_{2Z_0'} = -\frac{\Pr S f_2}{f_3}(M_0 - \alpha), K_{2Z_0'M_0} = -\frac{\Pr S f_2}{f_3}, K_{2Z_0'M_0'} = K_{2Z_0'M_0''} = 0,$

$K_{3E_0'} = -S\,Sc(M - \alpha), k_{2E_0'M_0} = -S\,Sc, K_{3M_0} = -S\,ScE_0', K_{3M_0E_0'} = -S\,Sc.$

Substituting Equations.22-30 in Equations.21a-21c, we obtain the following results solutions:

Results and Discussions:

In this section, the Impacts of various physical parameters on the axial velocity $M(\alpha)$, the radial velocity $M'(\alpha)$, temperature $Z(\alpha)$ and concentration $E(\alpha)$ distributions are analyzed . So to show the graphical and the tabular simulation, the results and discussions are divided into four in the upcoming subsections for $Pr = 6.2, Ec = \psi = 0.01$ as follows:

1-Tabular Discussion of Physical Quantities: The effects of S on the Sherwood number S_{hx}^* , the Nusselt number N_{ux}^*, and the skin-friction coefficient C_{fx}^* are shown in Table.2. Through this table it can watch clearly that N_{ux}^* and C_{fx}^* are oppositely proportional to S, while S_{hx}^* is directly proportional to S. The comparison between non-metallic nanoparticles (Al2O3, TiO2) and metallic nanoparticles (Ag, Cu) is demonstrated in the Table. 3. It is noted in the mentioned table that the value of the C_{fx}^* is less for metallic nanoparticles than non-metallic nanoparticles, but non-metallic nanoparticles have an increased mass and heat transfer rate compared to metallic nanoparticles. Table.4 displays the impacts of $C_{fx}^*, N_{ux}^*, S_{hx}^*$ and for several values of Kn . It can be seen from the table that the influence of growing K values is to reduce the rate of mass transfer , the rate of heat transfer , and the skin-friction coefficient. Further, the impacts of the nanoparticle volume fraction Δ are displayed in Table .5. From this table it is determined that the incrementing values Δ of rises C_{fx}^* and decreases the N_{ux}^*, S_{hx}^*. Table.6 displays the impacts for $C_{fx}^*, N_{ux}^*, S_{hx}^*$ for diverse values of slip number Ω and Schmidt number Sc. The impact growth of Ω is to rise the coefficient of skin-friction with decreasing the rate of mass and heat transfer may that noticed from this table. Furthermore , the rate of mass transfer growth with the rise in Sc, whereas the skin friction coefficient and the rate of heat transfer not have any influence when changing Sc on the rate of heat transfer and the skin friction coefficient .

Table.2: Calculating of C_{fx}^*, N_{ux}^* and S_{hx}^* various values of S for Cu$^{\text{water}}$ nano-fluid when $Kn = Sc = 1, \Delta = 0.02, \Omega = 0.1$.

S	-1.0	-0.5	0	0.5	1.0
C_{fx}^{*} [6]	-1.34295	-1.77787	-2,09419	-2.34148	-2.54426
C_{fx}^{*}	-1.70854	-1.97792	-2.19683	-2.37941	-2.53538
N_{ux}^{*} [6]	0.187977	0.127657	0.104693	0.094096	0.088577
N_{ux}^{*}	0.184680	0.113226	0.103595	0.093037	0.090204
S_{hx}^{*} [6]	-1.0694254	-1.0293233	-1.0000000	-0.9770841	-0.9583107
S_{hx}^{*}	-1.0618908	-1.0271843	-1.0000000	-0.9773102	-0.9574584

Table.3: The calculating of C_{fx}^*, N_{ux}^* and S_{hx}^* with various nanoparticles when $Kn = Sc = 1, \Delta = 0.02, \Omega = 0.1$.

Nanoparticle	Ag	Cu	TiO2	Al2O3
C_{fx}^{*} [6]	-2.48678	-2.54426	-2.73607	-2.74807
C_{fx}^{*}	-2.476075	-2.53581	-2.73309	-2.74591
N_{ux}^{*} [6]	0.088535	0.088577	0.088742	0.088792
N_{ux}^{*}	0.090147	0.090204	0.090906	0.090959
S_{hx}^{*} [6]	-0.95851	-0.95831	-0.95777	-0.95772
S_{hx}^{*}	-0.95751	-0.95746	-0.95703	-0.95700

Table.4: The calculating of C_{fx}^*, N_{ux}^* and S_{hx}^* various values of Kn for Cu^{water} nano-fluid when $S = Sc = 1, \Delta= 0.02, \Omega = 0.1$.

kn	C_{fx}^*[5]	C_{fx}^*	N_{ux}^*[5]	N_{ux}^*	S_{hx}^*[5]	S_{hx}^*
0	-2.46084	-2.43009	0.089198	0.090793	-0.95676	-0.95635
1	-2.54426	-2.50306	0.088577	0.090204	-0.95831	-0.95768
2	-2.62230	-2.57136	0.088075	0.088951	-0.95974	-0.95892

Table.5: The calculating of C_{fx}^*, N_{ux}^* and S_{hx}^* with various values of Δ for Cu^{water} nano-fluid when $Sc = S = Kn = 1, \Omega = 0.1$.

Δ	C_{fx}^*[5]	C_{fx}^*	N_{ux}^*[5]	N_{ux}^*	S_{hx}^*[5]	S_{hx}^*
0.00	-2.76550	-2.764221	0.092885	0.100352	-0.95773	-0.956968
0.02	-2.54426	-2.535381	0.088577	0.090204	-0.95831	-0.957458
0.05	-2.31844	-2.301882	0.082295	0.086806	-0.95911	-0.958051

Table.6: The calculating of C_{fx}^*, N_{ux}^* and S_{hx}^* with various values of Sc and s Ω for Cu^{water} nano-fluid when $Sc = S = Kn = 1, \Omega = 0.1$.

Sc	S_{hx}^*	Ω	C_{fx}^*	N_{ux}^*	C_{fx}^*
0	-1.000000000	0.01	-3.3242353	0.158907	-0.9431919
5	-0.777004441	0.09	-2.5739918	0.095350	-0.9564467
10	-0.472332473	0.10	-2.5030648	0.090204	-0.9576854

2-The Discussion of Tables: In order to certify the analytical outcomes obtained, in Table. 7 and Table. 8, exposed comparison of the present solutions, written report by Gupta and Ray[2] and Runge-Kutta-Fehlberg scheme of fourth-fifth order (RKF45)[5] and they found a good agreement for the axial velocity $M(\alpha)$ and temperature $Z(\alpha)$. Table.9 and Table.10 shown the comparison of the results with RK4S on the axial velocity $M(\alpha)$ and temperature $Z(\alpha)$ for two cases when $S > 0$ means the moving of plates apart and $S < 0$ leads to the moving of plates together. From these tables it can observe clearly the solution are a good match for both cases.

Table.7: The comparison the values of $M(\alpha)$ and $Z(\alpha)$ with RK4 for $S = 1, \Delta = 0.02, Pr = 6.2, Kn = SC = \Omega = 0$.

α	Gupta and Ray[2]	RKF45[5]	Present result
0.0	0.00000000	0.00000000	0.00000000
0.1	0.14135866	0.14135879	0.14136869
0.2	0.28066605	0.28066639	0.28068547
0.3	0.41578075	0.41578137	0.41580821
0.4	0.54437882	0.54437979	0.54441219
0.5	0.66385692	0.66385837	0.66389328
0.6	0.77122923	0.77123132	0.77126478
0.7	0.86301562	0.86301853	0.86304578
0.8	0.93511971	0.93512364	0.93513984
0.9	0.98269524	0.98270044	0.98270280
1.0	1.00000000	1.00000000	1.00000000

Table.8: The comparison the values of $M(\alpha)$ and $Z(\alpha)$ with RK4 for $S = 1, \Delta = 0.02, Pr = 6.2, Kn = SC = \Omega = 0$.

α	Gupta and Ray[2]	RKF45[5]	Present result
0.0	1.03206637	1.02996637	1.034179872
0.1	1.03206407	1.02996428	1.034147797
0.2	1.03203202	1.02993531	1.034147797
0.3	1.03189263	1.02980932	1.034008169
0.4	1.03150811	1.02946175	1.033621990
0.5	1.03066423	1.02869896	1.032769762
0.6	1.02903983	1.02723066	1.031113515
0.7	1.02615205	1.02462037	1.028127453
0.8	1.02125916	1.02019765	1.022978178
0.9	1.01318608	1.01290031	1.014325533
1.0	1.00000000	1.00000000	1.000000000

Table. 9: The comparison the values of $M(\alpha)$ and $Z(\alpha)$ with RK4 when $S = 0.3, \Delta = 0.02, Kn = 0.2, Pr = 0.2, SC = 0.1, \Omega = 0.1$.

α	$M(\alpha)$	RK4	$Z(\alpha)$	RK4
0.0	0.0000000000	0.000000000	1.000764038	1.000764038
0.1	0.1348198148	0.134820063	1.000763969	1.000763967
0.2	0.2676739026	0.267675168	1.000763009	1.000762881
0.3	0.3965666787	0.396573333	1.000758855	1.000758230
0.4	0.5194427132	0.519467467	1.000747514	1.000745769
0.5	0.6341564956	0.634225124	1.000723056	1.000719324
0.6	0.7384418402	0.738594877	1.000677232	1.000670417
0.7	0.8298808532	0.830167904	1.000598967	1.000587739
0.8	0.9058724075	0.906333150	1.000473649	1.000456402
0.9	0.9636001337	0.964224080	1.000282218	1.000256878
1.0	1.0000000000	1.000000000	1.000000000	1.000000000

Table. 10: The comparison the values of $M(\alpha)$ and $Z(\alpha)$ with RK4 when $S = -0.3, \Delta = 0.02, Kn = 0.2, Pr = 0.2, Sc = 0.1, \Omega = 0.1$.

α	$M(\alpha)$	RK4	$Z(\alpha)$	RK4
0.0	0.0000000000	0.0000000000	1.000968638	1.000968638
0.1	0.1408361219	0.1408358774	1.000968519	1.000968517
0.2	0.2790646202	0.2790651872	1.000966846	1.000966623
0.3	0.4121069915	0.4121147341	1.000959721	1.000958640
0.4	0.5374422752	0.5374775462	1.000940833	1.000937913
0.5	0.6526341027	0.6527447283	1.000901717	1.000895783
0.6	0.7553557098	0.7556358322	1.000832097	1.000822019
0.7	0.8434123108	0.8440273030	1.000720245	1.000705338
0.8	0.9147602618	0.9159785955	1.000553366	1.000533975
0.9	0.9675225258	0.969755602	1.000317945	1.000296286
1.0	1.0000000000	1.0000000000	1.000000000	1.000000000

3-The Discussion of Figures: Figures.3-8 display the behavior of the distributions for the axial velocity $M(\alpha)$, the radial velocity $M'(\alpha)$, temperature $Z(\alpha)$ and concentration $E(\alpha)$ with Cu/water nano-fluid varied values parameters. Figure. 3 demonstrates with increasing values Kn, the axial velocity decreases, and the radial velocity losses close the lower plate surface for $0 \le \alpha \le 0.5$, while after a confident distance the velocity rises when $\alpha \ge 0.5$. Obviously, this figure gives temperature drops monotonously for rising values of Kn. Also, the distinctions of the velocity and temperature for diverse values of volume fraction parameter are evidenced in Figure.4. It can be seen from the figure that it is similar to the case of increasing the parameter of the magnetic. Figure.5 depicts that the axial velocity decreases,

near the wall the values of the radial velocity decrease for $0 \leq \alpha \leq 0.6$ while for $0.6 \leq \alpha \leq 1$ the radial velocity increases and higher slip number values the temperature monotonically. From this figure that the concentration of $E(\alpha)$ with higher values of slip number Ω is dropping. When the base fluid is water, Figures.6 illustrates the impact of various nanoparticles on temperature and velocity. It has been established from this figure noted that titanium oxide TiO2 has a slightly higher distribution of velocity for different nano-fluids as compared with various other nanoparticles such as Cu, Ag, and Al2O3 which have different velocities. The radial velocity $M'(\alpha)$ is decreasing for $0 \leq \alpha \leq 0.5$, with the different nanoparticles while the outcomes become inverted for $0.5 \leq \alpha \leq 1$. It is noticed a review of this figure can matter of nano-fluid for reducing values of $Z(\alpha)$ while α alteration between 0 and 1 is TiO2/ water, Al2O/ water, Ag/ water and Cu/water nano-fluid, but the concentration values have no effect when changing the nanoparticle materials. The properties of S on concentration, temperature and velocity distributions are drawn in Figure.7. We can easily see from this figure the velocity values near the surface of the bottom plate decreases regularly with the increase of the value of S, and as we move away from the surface of the bottom plate, this values increases and increasing values of the squeeze number S appears decreases the temperature $Z(\alpha)$. Also, this figure demonstrates that the values of $E(\alpha)$ rise with higher squeeze number and increasing of α means a slight increment in the concentration $E(\alpha)$. Figure.8 demonstrates the effectiveness of rising the Schmidt number Sc in growing the concentration profile.
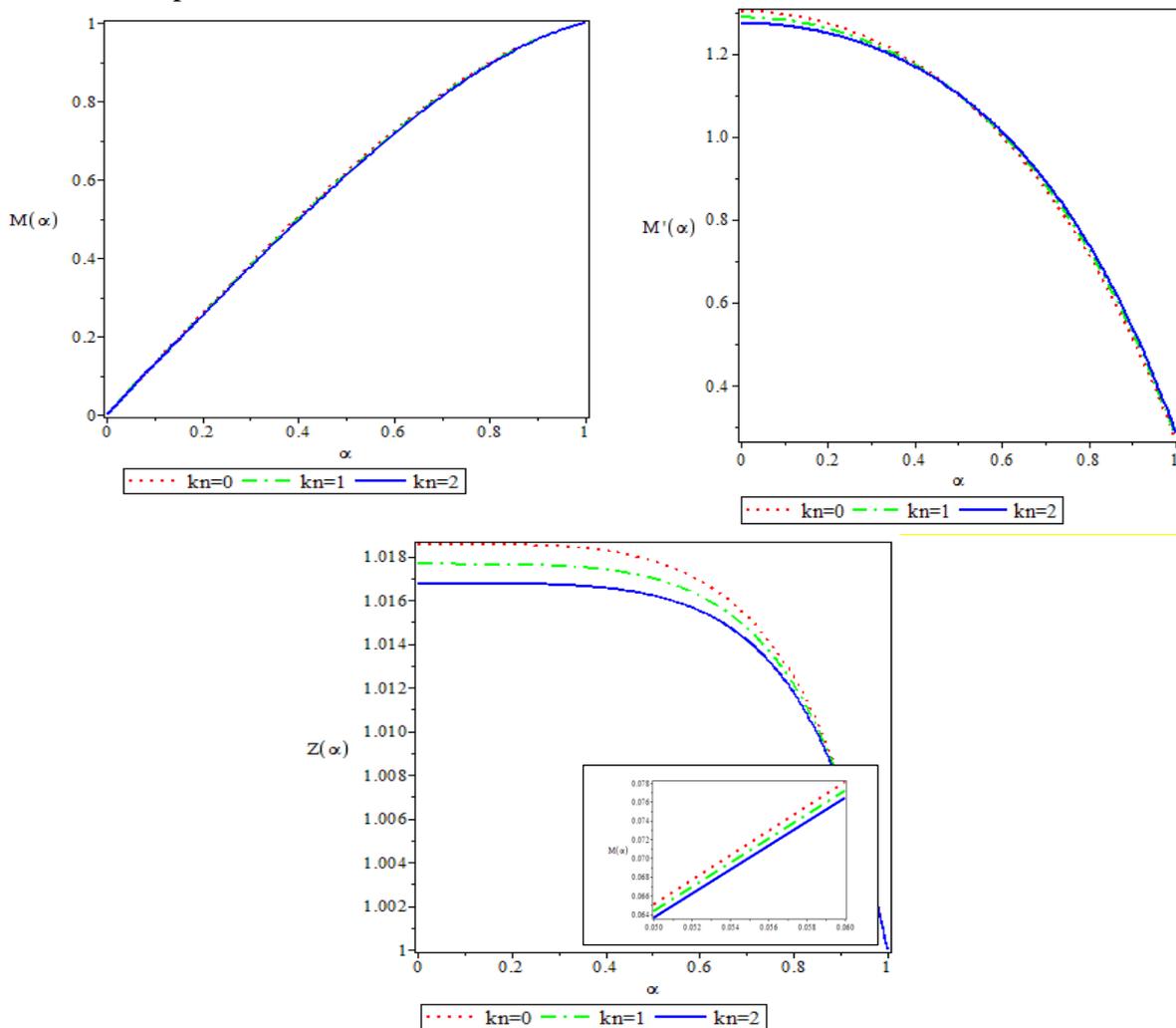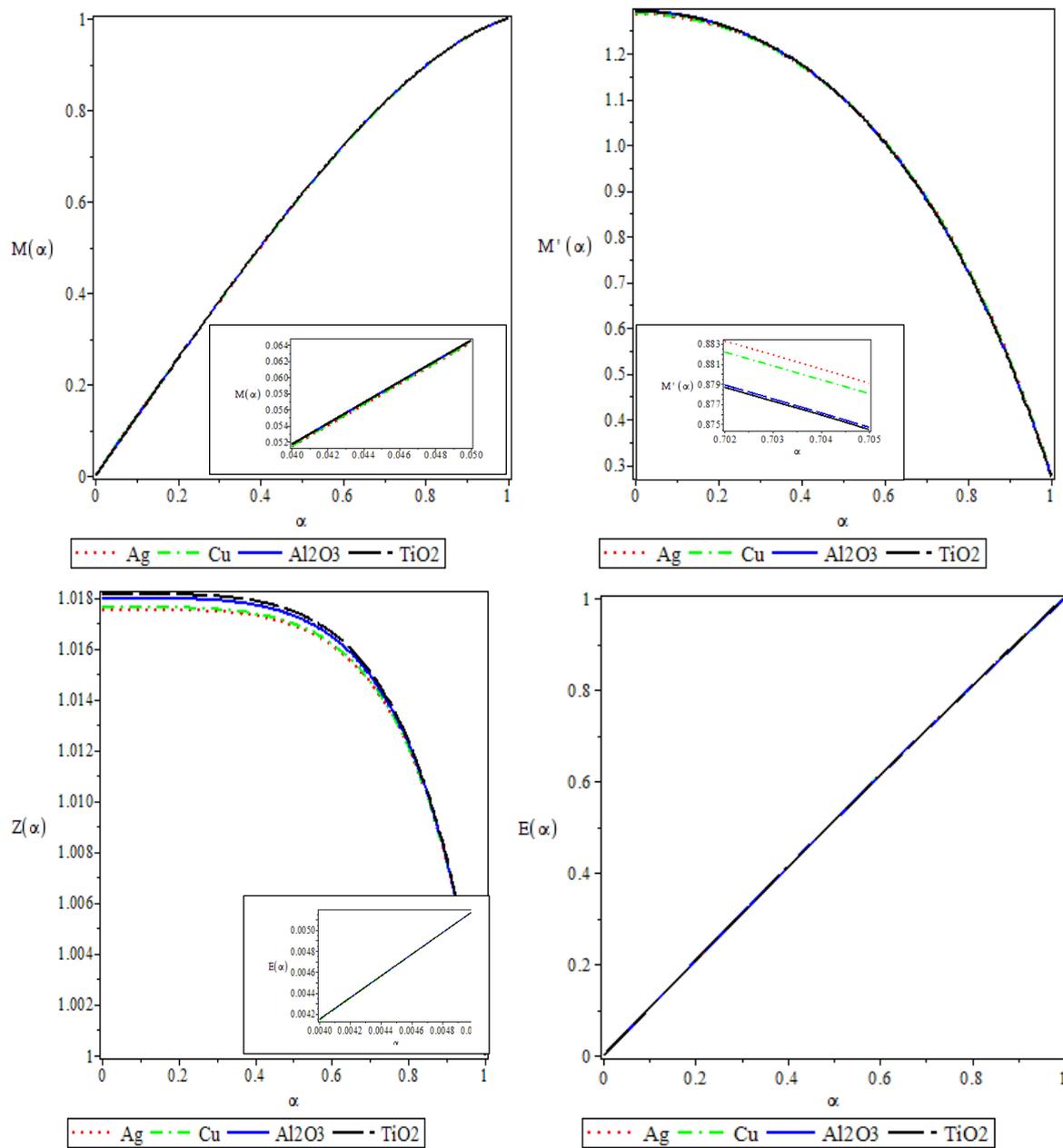

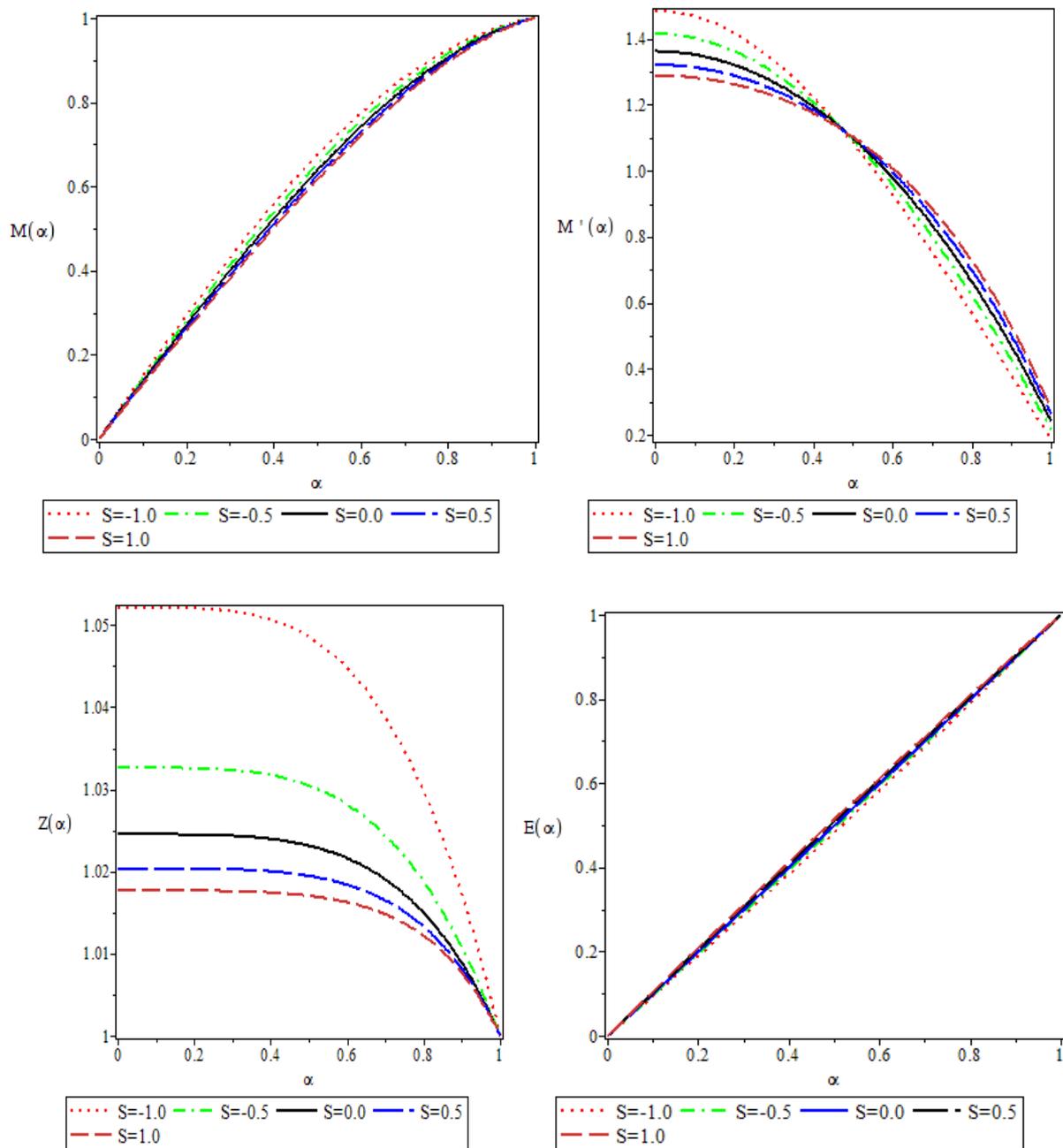**Figures 3:** The behavior kn on $M(\alpha), M'(\alpha)$ and $Z(\alpha)$.
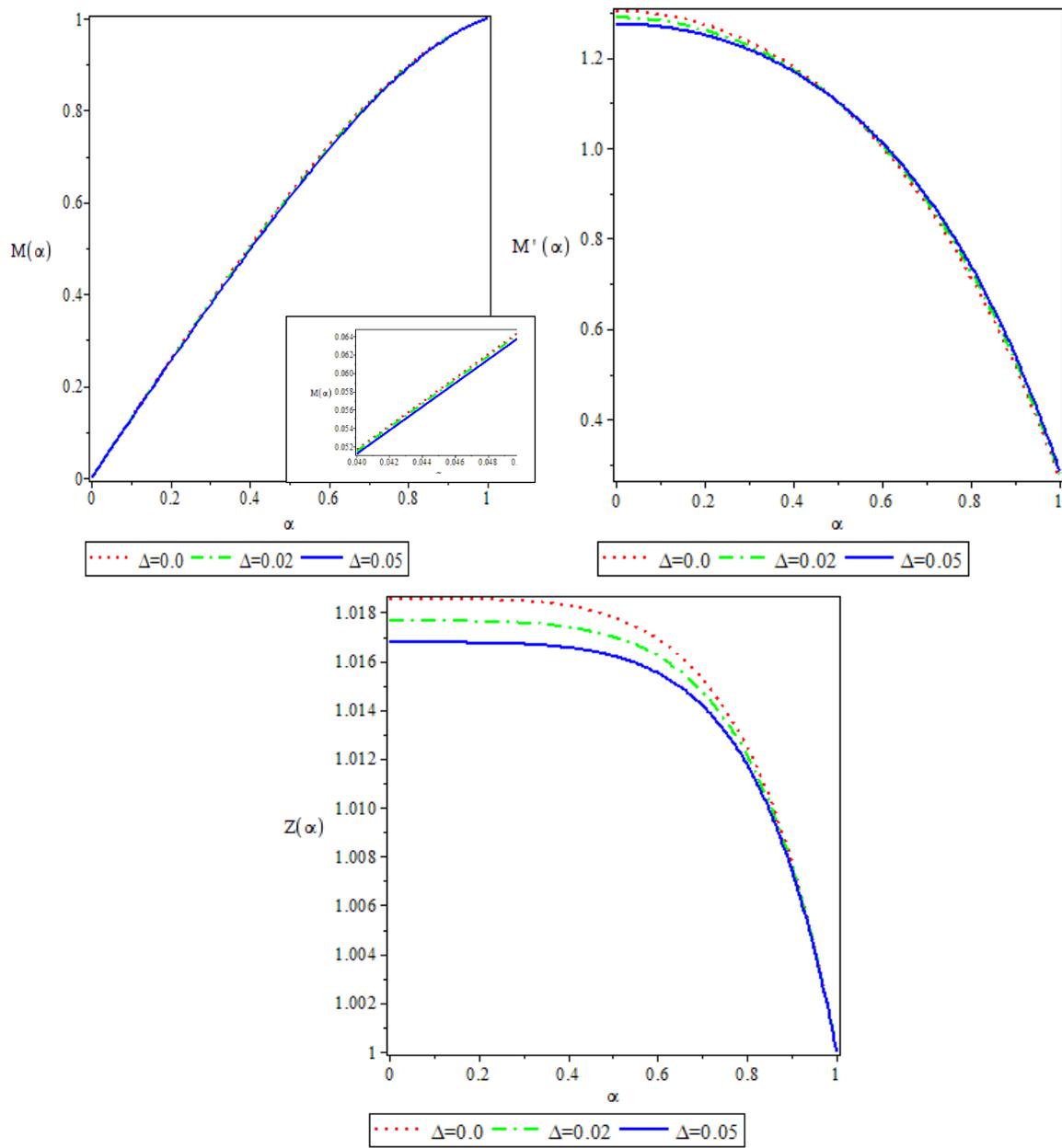
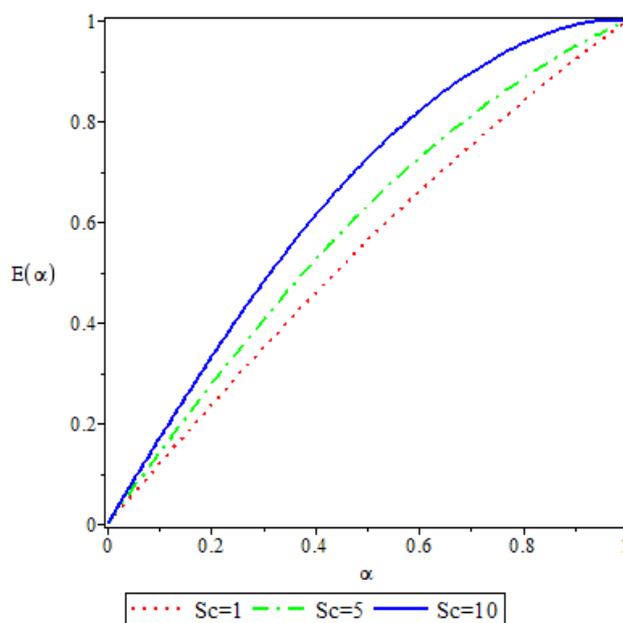**Figure 4:** The behavior Δ on $M(\alpha)$, $M'(\alpha)$ and $Z(\alpha)$.
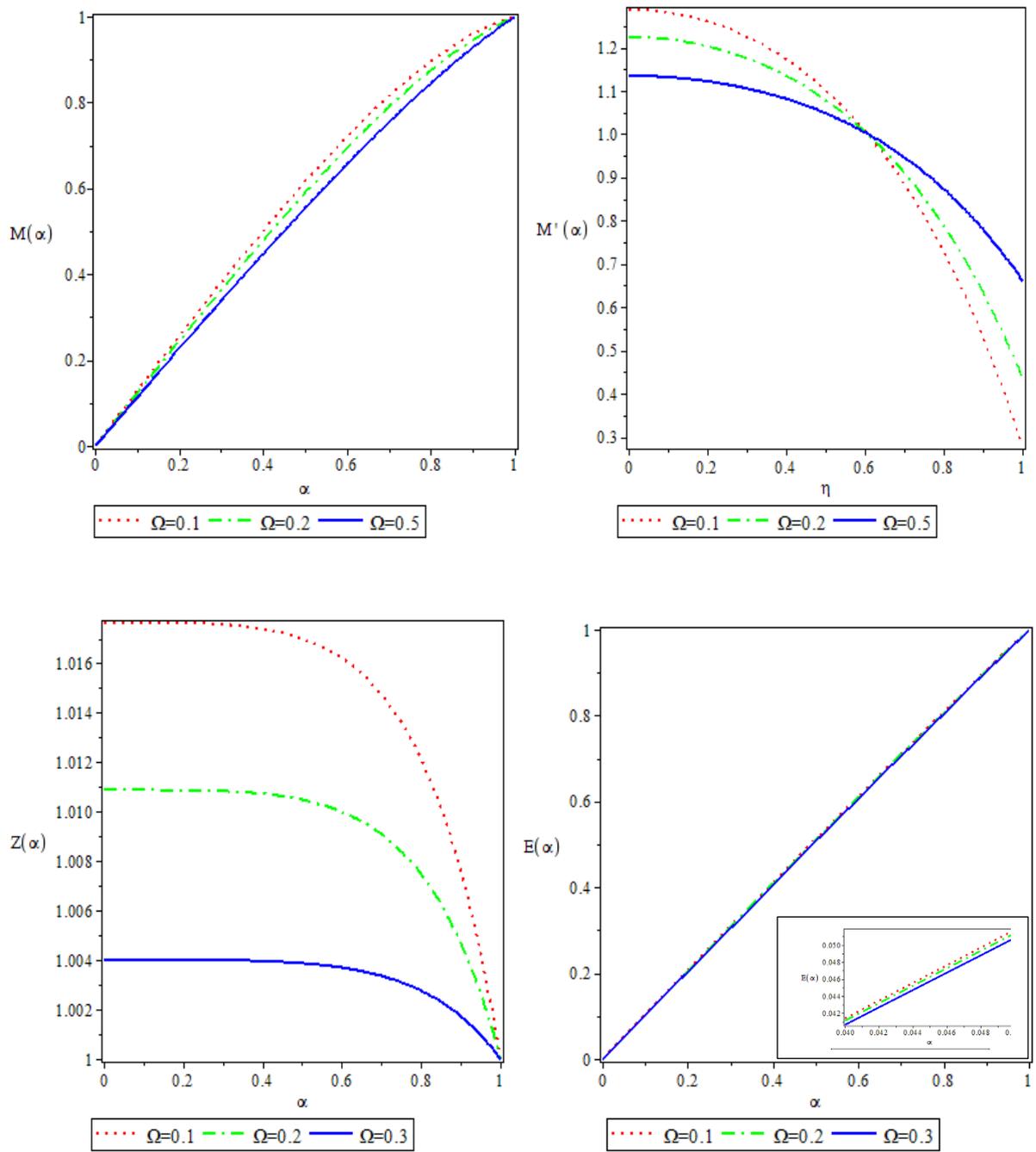
Figure 5: The behavior Ω on $M(\alpha), M'(\alpha), Z(\alpha)$ and $E(\alpha)$.

Figure 6 : The behavior nanoparticles on $M(\alpha), M'(\alpha), Z(\alpha)$ and $E(\alpha)$.

Figure 7 : The behavior S on $M(\alpha), M'(\alpha), Z(\alpha)$ and $E(\alpha)$.

Figure 8: The behavior Sc on $E(\alpha)$.

Conclusion:

The governing equations for this paper are a group of ordinary differential equations that result by using a proper transformation of the partial differential equations. The effect of slip velocity, addressing the current paper the analytical and numerical solutions incompressible viscous nano-fluid of two-dimensioned an unsteady magneto hydrodynamic flow among two parallel plates that are of infinite extension. In addition, The proposed problem are resolved numerically using fourth-order of the Runge-Kutta scheme. The above discussions provide outcomes are as follows:

(a) The rising of the magnetic field, in Cu-water nanofluid lead to The temperature distribution is dropping. The base fluid is H2O, the axial velocity of the nano-fluid with the nanoparticles of metallic Ag and Cu is lower than the nanoparticles of nonmetallic TiO2 and Al2O3, but after $\alpha = 0.5$ nature gives opposite. The temperature distribution of the nonmetallic nanoparticles is greater than the metallic nanoparticles.

(c) The temperature begins to drop in Cu-water nanofluid when the squeezing number positive .

(d) The raising values of Kn and S drive to the radial velocity $M'(\alpha)$ of Cu- water lows down normally in both cases it is opposite after $\alpha = 0.5$.

(f) For Cu- water nanofluid, the rate for heat transfer and the rate for mass transfer decrease as The squeezing number positive .

(e) The rate of heat transfer and the rate of mass transfer for the nanoparticles of metallic are minor than the nanoparticles of nonmetallic.

(g) As the squeeze number values increase, the concentration value increases slightly. Also the variable values of the slip parameter has little effect on the concentration.

(h) In concentration, the amount of improvement can be visible as Schmidt number goes up.

References:

[1] M. J. Stefan, "Versuch uber die scheinbare adhesion sitzungsbersachs Akademie der Wissenschaften in Wien," *Mathematisch- Naturwissenschaftliche Klasse*, vol. 69, pp. 713–721,1874.

[2] A. K. Gupta and S. S. Ray, " Numerical treatment for investigationof squeezing unsteady nanofluid flow between two parallel plates" , *Powder Technology*, vol. 279, pp. 282–289, 2015.

[3] S. U. S. Choi and J. A Eastman," Enhancing thermal conductivity of fluids with nanoparticle", *Proceedings of the International Mechanical Engineering Congress and Exhibition*, vol. 231, pp. 99–105, 1995.

[4] U. Khan, N.Ahmed, M. Asadullah, and S. T. Mohyud-din, " Effects of viscous dissipation and slip velocity on two-dimensional and axisymmetric squeezing flow of Cu-water and Cukerosene nanofluids," *Propulsion and Power Research*, vol. 4, no.1, pp. 40–49, 2015.

[5] S. Khilap, K. R. Sawan and K. Manoj, " Heat and mass transfer on squeezing unsteady MHD nanofluid flow between parallel plates with slip velocity effect" , *Journal of Nanoscience*, 2016.

[6] A. J. A. Al-Saif and A. M. Jasim, " Analytical Investigation of the MHD Jeffery-Hamel Flow Through Convergent and Divergent Channel by New Scheme" , *Engineering Letters*, 27:3, EL-27-3-28, 2019.

[7] A. M Jasim, " Analytical approximation of the first grade MHD squeezing fluid flow with slip boundary condition using a new iterative method", *Heat transfer*, PP.1-21,2020.

[8] A. M. Jasim, "New analytical study for nanofluid between two non-parallel plane palls (Jeffery-Hamel Flow)," *J. Appl. Comput. Mech*, vol.7 , no.1, pp. 213-224, 2021.

[9] A. M. Jasim, "Mean Square Analytical Solution for Beta Statistical Function with Second-Order Random Differential Equation", *Journal of Physics*, pp.1-13, 2020.

[10] A. J. A. Al-Saif and A. M. Jasim," A new analytical-approximate solution for thesqueezing flow between two parallel Plates", *Appl. Math. Inf. Sci.* , vol. 13, no.2, pp. 173-182,2019.

[11] A. M. Jasim and A. J. A Al-Saif, "New Analytical Solution Formula for Heat Transfer of Unsteady Two-Dimensional Squeezing Flow of a Casson Fluid between Parallel Circular Plates", *Journal of Advanced Research in Fluid Mechanics and Thermal Sciences,* vol. 64, no.2, pp.219-243,2019.

[12] Y. Q. Song, "Physical impact of thermo-diffusion and diffusion-thermo on Marangoni convective fow of hybrid nanofuid (MnZiFe2O4−NiZnFe2O4−H2O) with nonlinear heat," *Modern Phys. Lett. B*, vol.35, no.22, 2021.

[13] R. N. Kumar, "Impact of magnetic dipole on ferromagnetic hybrid nanofuid fow over a stretching cylinder," *Phy. Scripta*, vol. 96, 2021.

[14] Y. Q. Song, "Unsteady mixed convection fow of magneto-Williamson nanofuid due to stretched cylinder with signifcant non-uniform heat source/sink features", *Alex. Eng. J.,*vol. 61, pp.195–206 ,2022.

[15] R. J. Punith Gowda, R. N. Kumar and B. C. Prasannakumara, "Two-phase Darcy–Forchheimer flow of dusty hybrid nanofuid with viscous dissipation over a cylinder", *Int. J. Appl. Comput. Math,* vol. 7, no. 95 ,2021.

[16] S. A Khan, "Magnetic dipole and thermal radiation impacts on stagnation point flow of micropolar based nanofuids over a vertically stretching sheet: Finite element approach", *Processes*, vol. 9, no.1089 ,2021.

[17] S. A Khan, Y. Nie and B. Ali, "Multiple slip effects on magneto-hydrodynamic axisymmetric buoyant nanofuid flow above a stretching sheet with radiation and chemical reaction". *Symmetry*, vol. 11, no.1171, 2019.

[18] R. N. Kumar, "Comprehensive study of thermophoretic diffusion deposition velocity efect on heat and mass transfer of ferromagnetic fluid flow along a stretching cylinder", *J. Process Mech. Engr. Part E*, vol. 235, pp.1479–1489 , 2021.